Neutron-diffraction study of $ErBa_2Cu_3O_x$ in the composition range $6.1 \leq x \leq 7.0$

B. Rupp

Institut für Festkörperforschung, Kernforschungsanlage Jülich G.m.b.H., D-5170 Jülich, Federal Republic of Germany
and Labor für Neutronenstreuung, Eidgenössische Technische Hochschule Zürich,
Paul Scherrer Institut CH-5232 Villigen, Switzerland

E. Pörschke and P. Meuffels

Institut für Festkörperforschung, Kernforschungsanlage Jülich G.m.b.H., D-5170 Jülich, Federal Republic of Germany

P. Fischer and P. Allenspach

Labor für Neutronenstreuung, Eidgenössische Technische Hochschule Zürich,
Paul Scherrer Institut CH-5232 Villigen, Switzerland

(Received 28 December 1988; revised manuscript received 20 March 1989)

Structural properties of homogeneous orthorhombic and tetragonal $ErBa_2Cu_3O_x$ powder samples ($6.1 \leq x \leq 7.0$), prepared by a careful absorption-desorption procedure, were investigated by elastic neutron scattering. With decreasing oxygen content the distance between Cu(2)-O(2,3) planes and Cu(1)-O(4)-Cu(1) chains increases and the oxygen $2q(0,0,z)$ apex atoms O(1) move closer to the Cu-O-Cu chains. The copper-oxygen (1) distances do not vary continuously in the z direction but seem to change more rapidly when $x < 6.5$. The change of these distances can be correlated to the suppression of superconductivity in orthorhombic $ErBa_2Cu_3O_x$. A distinction between the large anisotropic vibrational amplitudes of the Cu(1)-O(4)-Cu(1) broken-chain oxygen atoms and a split-site model for O(4) is not possible on the basis of the present data.

I. INTRODUCTION

Substitution of Y by rare-earth (R) elements carrying a magnetic moment does not essentially affect the superconducting properties of high-T_c superconducting ceramics in the $RBa_2Cu_3O_x$ isostructural series.[1-3] Depending on their oxygen content, such materials show a remarkable variation of magnetic ordering on the R sites at low temperatures (see, e.g., Refs. 4 and 5). The smaller rare-earth elements have gained special interest as they allow one to investigate crystal-field splitting,[6] yielding additional information on the R-site local symmetry.

In previous work[7] we have successfully employed a defined oxygen sorption technique which enabled us to prepare large quantities of homogeneously loaded $RBa_2Cu_3O_x$ material covering the whole oxygen concentration range $6.0 \leq x \leq 7.0$. The aim to provide precise structural information on a consistently prepared set of well-characterized samples suitable for subsequent magnetic neutron scattering experiments and for crystal-field studies, motivated the present study of $ErBa_2Cu_3O_x$. Moreover, the monitoring of critical copper-oxygen distances might be essential for an understanding of the suppression of superconductivity in orthorhombic $RBa_2Cu_3O_x$ material.[8-10]

II. EXPERIMENTAL PROCEDURE

Polycrystalline single-phase starting material of $ErBa_2Cu_3O_x$ ($x \approx 7$) was prepared by a standard sintering procedure. We treated 12-g batches of powdered materi-

al by a temperature-controlled oxygen desorption-absorption procedure[7] and adjusted to yield final oxygen contents of $x = 6.10$, 6.35, 6.55, 6.65, 6.78, 6.87, and 7.0, respectively. The powdered samples were filled into vanadium cylinders of 10 mm diameter under helium atmosphere.

Neutron diffraction data were collected at 20 K on the multidetector powder diffractometer DMC at the SAPHIR reactor in Würenlingen, Switzerland [liquid-nitrogen-cooled Si filter, vertically focussing Ge(311) monochromator, collimation $10'/-/12'$, wavelength 1.7060(5) Å]. The diffraction patterns were refined employing the Rietveld method[11] using a modified form of a code by Hewat[12] including options for anisotropic temperature factor refinement adapted for 80286/87–CPU microcomputers.

III. RESULTS AND DISCUSSION

All neutron diffraction patterns could be completely indexed on the basis of the now well-established model of an orthorhombic or tetragonal tripled perovskite cell. No additional peaks of impurity phases with contributions larger than three e.s.d.'s of background could be observed nor did we detect any signs for weak systematic superstructure reflections due to long-range oxygen ordering. The magnetic structure of the Er sublattice is the subject of a study currently in progress at Institut Max von Laue-Paul Langevin (ILL) (Grenoble, France).[13]

A total of 165 (orthorhombic) or 100 (tetragonal) reflections were refined in the centrosymmetric space

groups *Pmmm* (No. 47, D_{2h}^1) or *P4/mmm* (No. 123, D_{4h}^1), respectively. A typical best fit for an orthorhombic refinement is shown in Fig. 1. Table I includes structural, occupational and thermal parameters as well as agreement factors R for all refinements. We follow the notation of the ILL group,[14] which corresponds to the Argonne description[15] if O(1) and O(4) are interchanged. Drawings of the basic crystal structure can be found in these papers. Occupation factors of O(4) chain atoms were refined in all runs; O(1), O(2), and O(3) showed only insignificant (2–3 e.s.d.'s) over and under occupation, which canceled out within the limited sensitivity of the Rietveld method, and were thus kept constant at 1.0 to avoid excessive parameter freedom. The absence of significant vacancies at the O(1) sites for samples prepared by our degassing-reloading method has been observed in highly oxygen deficient $YBa_2Cu_3O_x$ samples as well.[16] However, we wish to note that there might exist small real trends in occupational and thermal parameters beyond the accuracy of the standard Rietveld method. Inelastic scattering experiments sensitive to site symmetry of the central R atoms[6] might elucidate this problem.

In agreement with results for $YBa_2Cu_3O_x$ (Ref. 16) even in oxygen deficient orthorhombic material with low-x values we did not find indications for significant oxygen occupation at the O(5) 1b site ($\frac{1}{2},0,0$) on the a axis [i.e., if freely refined, oxygen occupations for O(5) became either negative within 1–3 e.s.d.'s or using fixed low positive occupation factors resulted in divergent B factors].

The profile parameters (U, V, W) derived for the samples were in the range usually observed for intermetallic powder specimens (using identical spectrometer configuration), i.e., they do not indicate anomalies in the diffraction peak width. Attempts to refine the sample
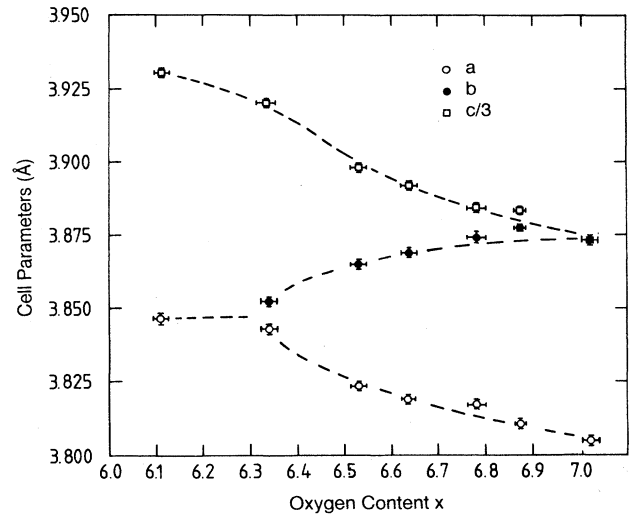

FIG. 2. Cell constants of $ErBa_2Cu_3O_x$ vs oxygen content (20 K). For $x = 7.0$, b and $c/3$ coincide. The dashed lines are guides to the eye only.

with $x = 6.34(2)$ into a tetragonal structure were not successful, i.e., if we tried to force significant oxygen occupation on the O(5) sites, the refinement diverged. In addition, the cell constants a and b did not refine to equal values. This result agrees with an extended x-ray study presented recently,[17] where the O-T transition was found at an oxygen concentration $6.25 < x < 6.30$. The large anisotropic thermal parameters of O(4) in oxygen deficient material might indicate that the chain oxygen atoms show already enhanced instability due to the close lying O-T phase transition. The cell constants of $ErBa_2Cu_3O_x$ versus oxygen content are shown in Fig. 2.
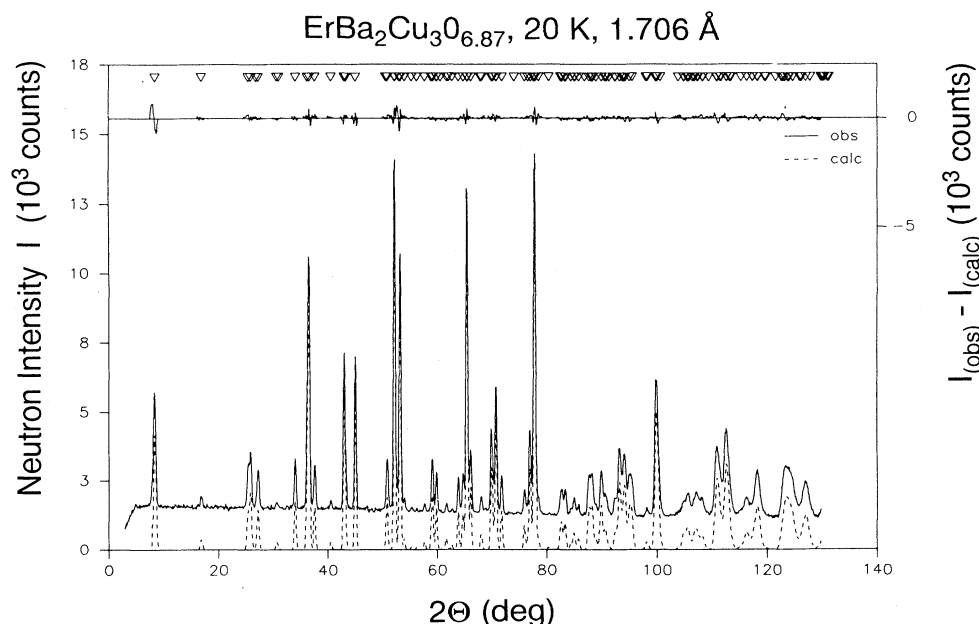

FIG. 1. Observed and calculated neutron diffraction profiles of $ErBa_2Cu_3O_{6.87}$ at 20 K, neutron wavelength 1.706 Å.

With decreasing oxygen content the O(1) atoms [apex of the dimpled square planar oxygen pyramides surrounding Cu(2)] move closer in z direction to the Cu(1) chain atoms and show somewhat enhanced, but still isotropic thermal vibrations. A similar trend was reported for quenched $YBa_2Cu_3O_x$ samples,[18] but in the latter case significant vacancies at the O(1) sites were observed. The variation of atomic distances between the O(1) apex atoms, the Cu(2) planes, and the Cu(1)-O(4) chains, respectively, are visualized in Figs. 3(a) and 3(b) (the chain-plane distance can be obtained from the sum of both distances quoted above). The error bars drawn in these figures do not reflect the usually too low standard devia-

tions obtained from the profile refinement output, but represent worst case estimates accounting for additional sources of errors like individual background subtraction, errors of cell constants, and errors of wavelength.

The most obvious features in the plots of copper-oxygen distances are the distinct decrease of the Cu(1)-O(1) distance and the distinct increase of Cu(2)-O(1) for $x < 6.5$. It is evident that these changes occur within the existence range of the orthorhombic phase. This observation is not specific for the $ErBa_2Cu_3O_x$ system; a similar behavior has been observed for $YBa_2Cu_3O_x$ as well, and led to speculations regarding the loss of superconductivity due to charge redistributions.[9,10,19] The Cu(1)-O(1)

TABLE I. Structural parameters of $ErBa_2Cu_3O_x$ at 20 K. For refined parameters the numbers in parentheses give the e.s.d.'s of the last significant digit; reliability factors were evaluated following the outlines of Young, Prince, and Sparks (Ref. 25). With the exception of the parameters of O(4), all refined parameters remained constant within e.s.d.'s, regardless of the structural model applied for the chain oxygen atoms O(4): (*) indicates isotropic model, (* *) stands for the split-site (static displacement) model, and all other values refer to the anisotropic temperature factor model. R values are listed for the anisotropic model only due to minor differences in R that can be evaluated only on the basis of a significance test checking for differences in the profile description. $ErBa_2Cu_3O_x$, space group $Pmmm$ [No. 47, D_{2h}^1, $x = 6.34$, 6.53, 6.64, 6.79, 6.87, 7.0; Er: $1h$, Ba: $2t$, Cu(1): $1a$, Cu(2), O(1): $2q$, O(2): $2s$, O(3): $2r$, O(4): $1e$, $2k$ (split site model)] or $P4/mmm$ [No. 123, D_{4h}^1, $x = 6.11$; Er: $1d$, Ba: $2h$, Cu(1): $1a$, Cu(2), O(1): $2g$, O(2)=O(3): $4i$, O(4): $2f$]. Neutron wavelength 1.7060(5) Å; temperature 20 K. Units for temperature factors B: Å^2. The form of temperature factors is isotropic: $\exp(-B_{iso}\sin^2\theta/\lambda^2)$ and anisotropic: $\exp[-(h^2a^{*2}B_{11}+k^2b^{*2}B_{22}+l^2c^{*2}B_{33})]$.

Atom	Parameter	6.11	6.34	6.53	6.64	6.78	6.87	7.0
Er	B	0.20(9)	0.32(8)	0.27(7)	0.32(8)	0.46(10)	0.22(7)	0.21(6)
Ba	B	0.02(9)	0.28(9)	0.19(9)	0.19(9)	0.07(11)	0.41(8)	0.30(6)
	z	0.1951(4)	0.1935(3)	0.1899(3)	0.1882(4)	0.1864(5)	0.1852(4)	0.1838(3)
Cu(1)	B	0.21(9)	0.20(8)	0.27(8)	0.12(8)	0.14(10)	0.10(7)	0.00(6)
Cu(2)	B	0.01(6)	0.10(5)	0.08(5)	0.11(6)	0.34(7)	0.04(5)	0.07(4)
	z	0.3610(3)	0.3609(3)	0.3584(3)	0.3575(3)	0.3567(4)	0.3565(2)	0.3552(2)
O(1)	B	0.35(9)	0.62(8)	0.41(8)	0.39(9)	0.39(12)	0.16(8)	0.30(7)
	z	0.1532(4)	0.1536(4)	0.1559(4)	0.1569(4)	0.1578(5)	0.1584(3)	0.1586(4)
O(2)	B	0.13(6)	0.05(22)	0.11(9)	0.04(9)	0.01(10)	0.13(7)	0.29(6)
	z	0.3797(3)	0.3828(6)	0.3802(5)	0.3796(5)	0.3782(6)	0.3785(4)	0.3779(3)
O(3)	B		0.34(6)	0.31(8)	0.17(9)	0.21(11)	0.18(7)	0.24(6)
	z		0.3792(2)	0.3770(3)	0.3770(5)	0.3770(6)	0.3789(4)	0.3790(3)
O(3)	B		0.05(22)	0.11(9)	0.04(9)	0.01(10)	0.13(7)	0.29(6)
	z		0.3828(6)	0.3802(5)	0.3796(5)	0.3782(6)	0.3785(4)	0.3779(3)
O(4)	B^*	1.5(9)	5.8(1.3)	2.5(5)	2.5(4)	2.2(4)	1.6(2)	1.2(2)
	B_{11}		6.3(1.8)	2.9(9)	3.8(9)	4.7(9)	2.4(4)	1.0(3)
	B_{22}		0.2(1.2)	1.7(7)	1.4(7)	0.5(6)	1.1(4)	1.0(3)
	B_{33}		6.4(2.0)	3.2(1.2)	2.7(1.1)	2.1(1.0)	1.3(4)	1.7(3)
	B^{**}		4.6(1.6)	2.3(6)	2.0(5)	1.2(5)	1.2(3)	1.1(2)
	x^{**}		0.049(27)	0.024(18)	0.038(10)	0.050(7)	0.030(7)	0.011(3)
	n	0.11(2)	0.34(2)	0.53(2)	0.64(2)	0.78(2)	0.87(1)	1.02(2)

				Cell constants (Å)				
a		3.846(2)	3.844(1)	3.823(1)	3.820(1)	3.817(2)	3.812(1)	3.803(1)
b			3.851(1)	3.865(1)	3.869(1)	3.874(3)	3.877(1)	3.873(1)
c		11.792(6)	11.760(5)	11.694(5)	11.676(5)	11.653(6)	11.650(5)	11.620(4)

				R values				
R_i		4.15	4.54	3.66	5.01	6.71	4.10	4.09
R_{wp}		10.02	9.06	8.19	9.09	10.96	7.69	7.50
R_e		4.18	4.03	4.20	4.53	5.03	4.17	3.92

distances, which represent also the shortest bond lengths in the $RBa_2Cu_3O_x$ structure, have been suggested to be an important parameter reflecting the local electronic environment.[10] The interpretation of a plot of Cu(1)-O(1) versus oxygen content, however, requires some caution. As the structural parameters of $RBa_2Cu_3O_x$ are known to be sensitive to the sample preparation technique, a compilation of data from various sources[19] might not reveal small but distinct secondary structural effects. We assume that our consistently prepared set of samples delivers results which are at least free from production-induced errors. As yet, however, we do not feel safe to draw in Figs. 3(a) and 3(b) either continuously, monotonic changing curves (see, e.g., Ref. 19) or discontinuous curves abruptly dropping for $x < 6.5$. What we need in

order to allow a nonambiguous interpretation are more data in the range $6.0 < x < 6.5$. We are currently collecting these data in the system $NdBa_2Cu_3O_x$. In Fig. 3(c), however, we have plotted the transition temperatures taken from Refs. 8 and 17 in addition to the corresponding Cu(1)-O(1) distances from Fig. 3(b) on a common scale. The shape of the curves is surprisingly similar, and a plot of T_c versus Cu(1)-O(1) yields a fairly linear correlation of T_c with the Cu(1)-O(1) distance (Fig. 4). For the $ErBa_2Cu_3O_x$ system, a limiting Cu(1)-O(1) distance of about 1.805(5) Å for the occurrence of superconductivity may be estimated. A very similar correlation was observed for a system $YBa_2Cu_{3-x}Co_xO_{7-y}$;[10] for such an electronically different system, however, quantitative differences, i.e., a more rapid suppression of T_c and a
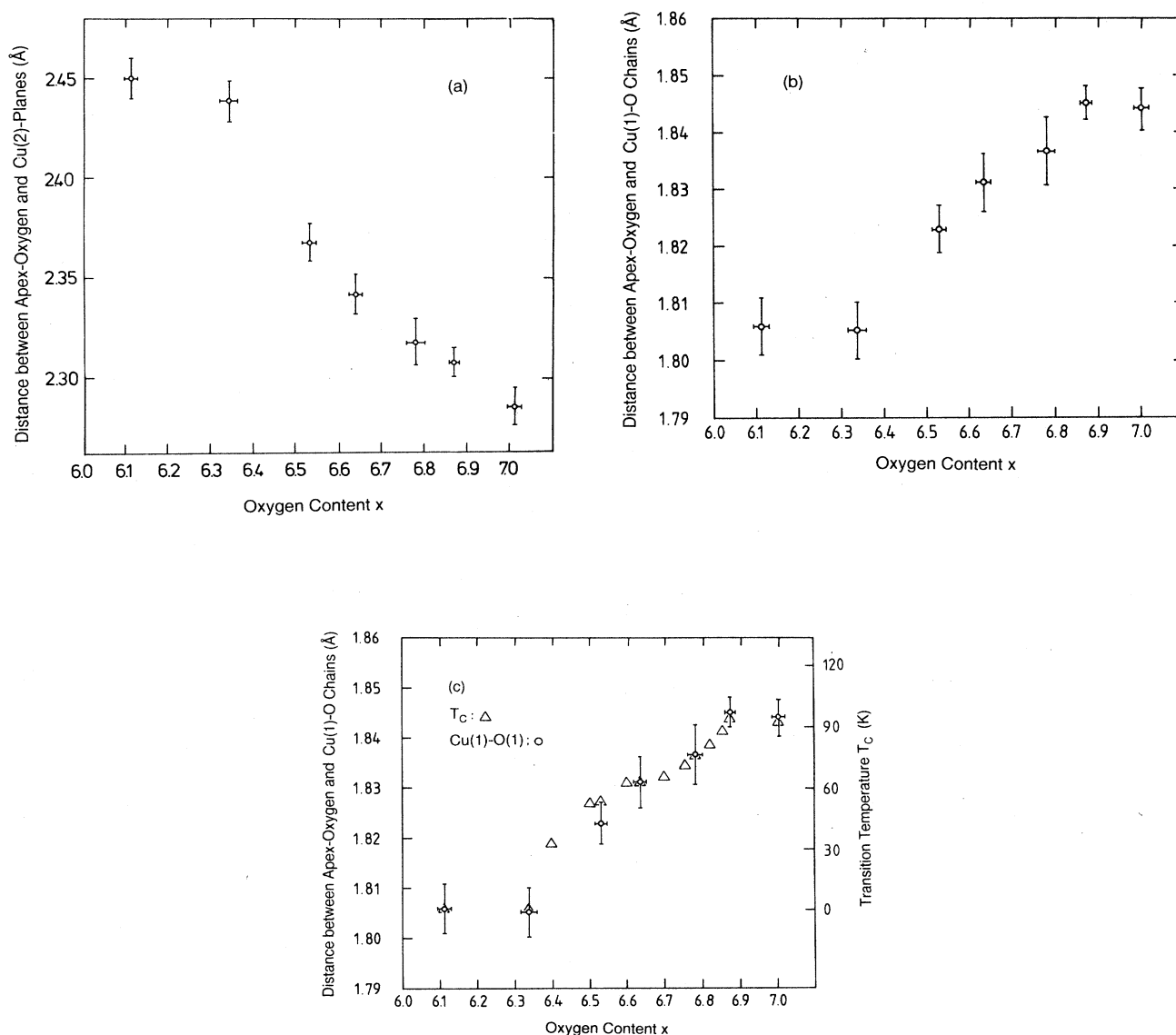
FIG. 3. Interatomic distances in $ErBa_2Cu_3O_x$: (a) distance between apex oxygen atom O(1), (0,0,z), and Cu(2) planes; (b) distance between apex oxygen atom O(1) and Cu(1) (chain site) atoms. In tetragonal cases the basal plane is statistically occupied with x minus 6.0 Cu atoms on the a and b axis. In (c) the transition temperatures are plotted in addition to the Cu(1)-O(1) distances.
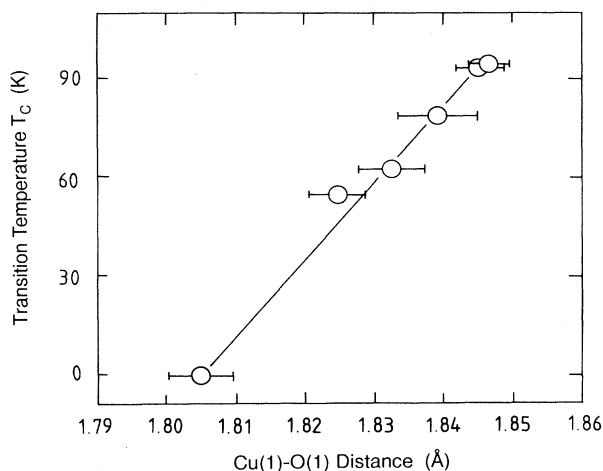
FIG. 4. Transition temperature of $ErBa_2Cu_3O_x$ as a function of Cu(1)-O(1) distance. The transition temperatures are onset values of dc-susceptibility measurements.[8,17]

larger limiting Cu(1)-O(1) distance (about 1.82 Å), are not surprising.

Based on the larger set of experimental neutron diffraction results on $ErBa_2Cu_3O_x$, we have extended in other papers[8] the electronic approach[9,10] using a charge-redistribution model for the electronic transfer from the Cu(1)-O chains to the Cu(2)-O planes, leading to a reduced hole concentration in the Cu(2)-O planes.

For oxygen-deficient orthorhombic material the temperature factors for the O(4) atoms are high and the thermal vibrations are anisotropically enhanced in the x direction. The large B_{11}'s of O(4) suggest an alternative approach using a split-site model, i.e., displacing the O(4) oxygen atoms from their position on the straight Cu-O-Cu broken chains along the b axis from the $1e$ $(0,\frac{1}{2},0)$ to a $2k$ site $(\pm x,\frac{1}{2},0)$, using small x values and an isotropic B factor.[20] For oxygen-deficient material the arrangement of the oxygen atoms is not expected to be an ordered zig-zag pattern due to the oxygen vacancies at these sites. In fact, any indications for a superstructure along the b axis are lacking in our patterns.

We have implemented a significance test, searching for differences in the predictions of the models similar to the algorithm used by Prince.[21] We obtained that (with exception of material with $x = 6.78$, which generally yielded a worse refinement and thus showed no significant differences between the models at all) at a confidence level of 90% the split-site model as well as the anisotropic model are significantly better than an isotropic model; the anisotropic model and the split-site model differ only insignificantly. This result is not unexpected in view of the difficulty to distinguish between anisotropic B's and a static displacement by means of elastic scattering techniques (see, e.g.,[22] for a discussion). Even from extended temperature-dependent studies of the anisotropic temperature factors and the static displacements of O(4) in the x direction,[20] it is difficult to derive a conclusive argument in favor of one of the two models in question. We have discussed the mean-square displacement and the corre-

sponding vibrational frequencies in detail in a previous paper[16] on $YBa_2Cu_3O_x$ material, where we have suggested that the good agreement with observed thermal modes[23] supports the anisotropic model.

The superconducting properties of pressed $ErBa_2Cu_3O_x$ powder as a function of oxygen content were investigated employing a superconducting quantum interference device (SQUID) magnetometer as well as ac-susceptibility measurements. The experiments were extended to a large set of about 20 samples, and are discussed in detail in other papers.[8,17] The overall picture is consistent with reports of other workers, and one can distinguish regions of sharp transitions at about 90 and 60 K, respectively, and broad transitions in the intermediate region and below $x < 6.5$. The most interesting result is that superconductivity becomes totally suppressed even in orthorhombic samples, and that this suppression does not coincide with the O-T phase transition. It should also be noted that sample $x = 6.78$, which is located in the region of broad superconducting transitions, yielded a significantly worse refinement compared to the other samples. Microscopic short-range order-disorder or microscopic phase separations, as discussed in Ref. 24, might account for this correlation.

IV. CONCLUSIONS

Our degassing-reloading procedure introduced earlier[7] efficiently allows access to material located in the low-oxygen part of $RBa_2Cu_3O_x$ pseudobinary phase diagrams. Neutron diffraction data show that the most striking structural effect on approaching low-equilibrium oxygen concentrations is a drastic change in the distance between the O(1) apex atoms and the Cu(2) planes and the Cu(1)-O(4) chains, respectively, for $x < 6.5$. The O(1) apex atom, which is located between the Cu-O chains and the Cu-O planes, might play an important role in a charge transfer mechanism between the Cu-O planes and the Cu-O chains. The suppression of superconductivity does not coincide with the O-T phase transition but correlates linearly with the decrease of Cu(1)-O(1) distances, supporting an all-electronic mechanism for oxide superconductivity.[8-10] The O(4) atoms show enhanced anisotropic vibrations perpendicular to the b axis, which can be equivalently described in terms of static displacements from the ideal position on the b axis. From profile refinements alone we cannot extract a conclusive decision between the split site or the anisotropic model. The need for precise structural information on well-prepared homogeneous samples cannot be overemphasized: In combination with extended investigations of the superconducting properties one might be able to establish the role of secondary structural effects in the mechanism of superconductivity in layered copper-oxide compounds.

ACKNOWLEDGMENTS

[1]F. Hulliger and H. R. Ott, Z. Phys. B **67**, 291 (1987).

[2]G. Xiao, F. H. Streitz, A. Gavrin, and C. L. Chien, Solid State Commun. **63**, 817 (1987).

[3]J. M. Tarascon, W. R. McKinnon, L. H. Greene, G. W. Hull, and E. M. Vogel, Phys. Rev. B **36**, 226 (1987).

[4]J. W. Lynn and W. H. Li, J. Appl. Phys. **64**, 6065 (1988).

[5]T. Chattopadhyay, P. E. Brown, D. Bonnenberg, S. Ewert, and H. Maletta, Europhys. Lett. **6**, 363 (1988).

[6]A. Furrer, P. Brüesch, and P. Unternährer, Phys. Rev. B **38**, 4616 (1988); P. Allenspach, A. Furrer, P. Brüesch, R. Marsolais, and P. Unternährer, Physica C **157**, 58 (1989).

[7]P. Meuffels, B. Rupp, and E. Pörschke, Physica C **156**, 441 (1988).

[8]H. Maletta, E. Pörschke, B. Rupp, and P. Meuffels, Z. Phys. B (to be published); P. Allenspach, A. Furrer, and B. Rupp, Proceedings of the International Seminar on High Temperature Superconductivity, Dubna, U.S.S.R., 1989 (World Scientific, Singapore, in press).

[9]R. J. Cava, B. Batlogg, K. M. Rabe, E. A. Rietman, P. K. Gallagher, and L. W. Rupp, Physica C **156**, 523 (1988).

[10]P. F. Miceli, J. M. Tarascon, L. H. Greene, P. Barboux, F. J. Rotella, and J. D. Jorgensen, Phys. Rev. B **37**(10), 5932 (1988).

[11]H. M. Rietveld, J. Appl. Cryst. **2**, 65 (1969).

[12]A. W. Hewat, Atomic Energy Research Establishment Report No. AERE-R7350, 1973 (unpublished); B. Rupp, MS-DOS microcomputer version (1988) (unpublished).

[13]H. Maletta, T. Chattopadhyay, P. J. Brown, and E. Pörschke (unpublished).

[14]A. W. Hewat, J. J. Capponi, C. Chaillout, M. Marezio, and E. A. Hewat, Solid State Commun. **64**, 301 (1987).

[15]J. D. Jorgensen, B. W. Veal, W. K. Kwok, G. W. Crabtree, A. Umezawa, L. J. Nowicki, and A. P. Paulikas, Phys. Rev. B **36**, 5731 (1987); J. D. Jorgensen, M. A. Beno, D. G. Hinks, L. Soderholm, K. J. Volin, R. L. Hitterman, J. D. Grace, I. K. Schuller, C. U. Segre, K. Zhang, and M. S. Kleefisch, *ibid.* **36**, 3608 (1987).

[16]B. Rupp, P. Fischer, E. Pörschke, R. R. Arons, and P. Meuffels, Physica C **156**, 559 (1988).

[17]E. Pörschke and P. Meuffels, in Proceedings of the European Materials Research Society Fall Meeting, Strassbourg, France, 1988 [J. Less-Common Met. **150**, 153 (1989)].

[18]W. K. Kwok, G. W. Crabtree, A. Umezawa, B. W. Veal, J. D. Jorgensen, S. K. Malik, L. J. Nowicki, A. P. Paulikas, and L. Nunez, Phys. Rev. B **37**, 106 (1988).

[19]M.-H. Whangbo, M. Evain, M. A. Beno, U. Geiser, and J. M. Williams, Inorg. Chem. **27**, 467 (1988).

[20]M. Francois, A. Junod, K. Yvon, P. Fischer, J. J. Capponi, P. Strobel, M. Marezio, and H. W. Hewat, Solid State Commun. **66**, 1117 (1988); Physica C **153-155**, 962 (1988).

[21]E. Prince, Acta Crystallogr., Sect. B **38**, 1099 (1982).

[22]G. Kartha and F. R. Ahmed, Acta Crystallogr. **13**, 532 (1970).

[23]P. Brüesch and W. Bührer, Z. Phys. B **70**, 1 (1988); and W. Bührer, P. Brüesch, P. Unternährer, and A. Taylor, Physica C **153-155**, 300 (1988).

[24]D. J. Werder, C. H. Chen, R. J. Cava, and B. Batlogg, Phys. Rev. B **38**, 5130 (1988).

[25]R. A. Young, E. Prince, and R. A. Sparks, J. Appl. Cryst. **16**, 357 (1982).